# Bright sources under the projection microscope: using an insulating crystal on a conductor as electron source

L Lapena, D Bedrane, A Degiovanni, E. Salançon

# Bright sources under the projection microscope: using an insulating crystal on a conductor as electron source

L. Lapena, D. Bedrane, A. Degiovanni, and E. Salançon

CINaM, Aix-Marseille Univ, CNRS, UMR 7325, France

November 20, 2021

## Abstract

The development of bright sources is allowing technological break-throughs, especially in the field of microscopy. This requires a very advanced control and understanding of the emission mechanisms. For bright electron sources, a projection microscope with a field emission tip provides an interference image that corresponds to a holographic recording. Image reconstruction can be performed digitally to form a "real" image of the object. However, interference images can only be obtained with a bright source that is small: often, an ultra-thin tip of tungsten whose radius of curvature is of the order of $10nm$. The contrast and ultimate resolution of this image-projecting microscope depend only on the size of the apparent source. Thus, a projection microscope can be used to characterize source brightness: for example, analyzing the interference contrast enables the size of the source to be estimated. Ultra-thin W tips are not the only way to obtain bright sources: field emission can also be achieved by applying voltages leading to a weak macroscopic electric field ($< 1V/\mu m$) to insulating micron crystals deposited on conductors with a large radius of curvature ($> 10\mu m$). Moreover, analyzing the holograms reveals the source size, and the brightness of these new emitters equals that of traditional field emission sources.

## 1 Introduction

Using a bright source is essential in microscopy applications. Moreover, the wave-like nature of particles is best observed using a bright source. It is only after the invention of the laser that the holography described and demonstrated by D. Gabor [1] was really implemented. Brightness corresponds to the emitted intensity at a given energy $I(E)$ under an angle of cone $\Omega$ coming from a zone $s$ on the source itself: $B = \frac{I(E)}{s\Omega}$. For a given intensity, the smaller the source, the brighter it is and the more spatially coherent the beam. A thermo-electronic electron source such as a heated filament, although very intense, cannot match the brightness of field emission sources such as an ultra-thin tungsten tip: the emission area is much too large. The tips may end with only a few atoms.

All the intensity comes from an extremely small area. The brightness is three orders of magnitude higher than a filament source [2]. A more recent example is the Helium ion source used in the Helium microscope. N.P. Economou et al. [3] explain the various obstacles that had to be overcome before using these sources in an ion column to reach resolutions of 0.35nm on the sample. The contrasts obtained in this microscope are unequaled. It took 20 years to go from the tungsten trimer to the reliable and reproducible beam. The first studies on these emitters were carried out with a field ion microscope. We will see in this article that a projection microscope is perfectly suited to characterizing sources and in particular their size, whatever the emitted particles [4, 5]. An electron source consisting of an insulating crystal deposited on a carbon fiber, as described in several articles [6, 7, 8, 9, 10], was characterized with these methods and will be described here.

## 2 Source-size measurement in a projection microscope

The projection microscope is a derivative of the field ion or field electron microscope, where only the emission profile and the structure of the emitter itself are observed. Instead of using a diaphragm as an extractor, the projection microscope uses an "open object" such as a lacey or holey carbon film deposited on a copper grid. The image of the object is then projected onto a screen. Being open, the lacey or holey carbon grids let the beam pass through them directly; their dimensions also vary, and they can be as small as a few nm [11]. In order to position the object precisely in front of the source, it is placed on a piezoelectric manipulator. The detector usually consists of one or more micro-channel plates (MCP) and a fluorescent screen. The amplification depends on the number of MCP and the voltage applied to the MCP stack. The resolution of the detector in analog mode is about $100\mu m$, but in particle-counting mode it is reduced to the plate pitch, i.e. about $15\mu m$ [8]. The image obtained with this type of microscope depends on the nature of the particles emitted, even at equivalent magnifications. The magnification factor is the ratio of the source-to-screen distance, $D$, to the source-to-object distance, $d$: $G = \frac{D}{d}$. The object is first positioned far from the source. From the grid pitch, the magnification can be determined precisely. Then, the object is moved closer and magnification gradually increases. Depending on the particle and the dimensions, fringes can be observed. In the case of a point source facing a point object, the position of the constructive fringes is calculated as follows: $x_p = G\sqrt{2p\lambda d}$ with $\lambda = \frac{h}{\sqrt{2mE}}$ the wavelength associated with the particle of mass $m$ and energy $E$ ($h$ is the Planck constant) and $p$ the interference order. For an electron emitted at 100V, the wavelength is 1.2 Å. If the object is $100\mu m$ from the source, in a 1m projection microscope, the first fringe is 1.55mm from the center and then the fringes get closer and closer. For ions, even when very light, such as hydrogen ions of 1keV, the wavelength is then 0.9pm and the first fringe is $134\mu m$ from the center. In a projection set-up with metric dimensions, no fringe will be seen in analog detection mode. Observations of fringes depends on the square root of the wavelength ratio $\sqrt{\frac{\lambda_e}{\lambda_{ions}}}$: if the wavelength is 100 times smaller, the projection distance must be 10 times greater to observe the same effect. Source size

is characterized via the projection microscope according to the contrast on the image, but the treatment is particle-dependent.
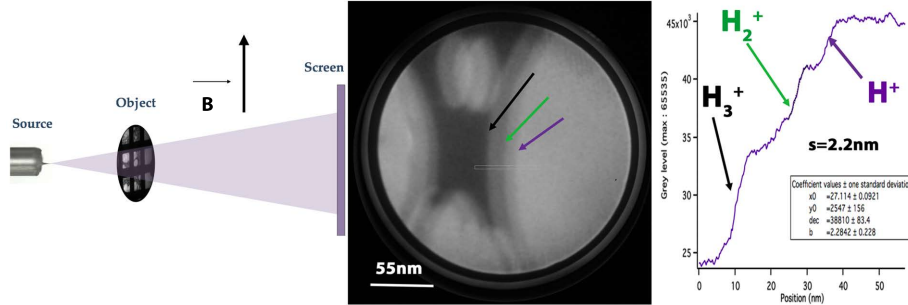


Figure 1: The size of the ion source is determined by measuring the contrast at the edge of the shadow of an object. Magnification: $G = 180000$, ion source potential $V = 2kV$, source-screen distance $D = 40cm$, source-object distance $d = 2.2\mu m$

In the case of ion sources, because no fringes are observed in our set-up, the contrast can be measured directly. Using the error function, the smallest observable detail is measured and corresponds to the maximum size of the source used to produce that image. In figure 1, the size of the coaxial ion source, presented in various articles [12, 13] is measured. The different species are first separated with a magnetic field ($H^+$, $H^{2+}$, and $H^{3+}$) and analyzed separately: the size of each ion source is about $s = 2.2nm$.

In the case of electron sources, the contrast cannot be measured directly because fringes are observed. To measure the source size for electrons, two methods are used: the last visible fringe [9], and the contrast in an interferometry experiment [14].

- The last visible fringe (at $x_{p_l}$) corresponding to the smallest visible detail is measured; the source is smaller than: $s < \frac{x_{p_l} - x_{(p_l-1)}}{2G} = \sqrt{\frac{\lambda d}{8p}}$. To determine source size $s < 10nm$, the image needs to be sufficiently magnified: in a $D = 1m$ projection microscope, the source-object distance has to be smaller than $d < 1\mu m$. In the case of an ultra-thin metal tip, this is a common requirement. However, if the support of the source is too bulky, as with the so-called "celadonite source" [9], it is impossible to respect this distance without touching the extractor grid. To overcome this difficulty, an electrostatic lens can be used to enlarge the fringe recording. In the example of figure 2, source size is estimated to be below $s < 2.6nm$. This recording corresponds to the first step of holography. A digital reconstruction procedure can be applied to find the shape of the object [15, 16]. With more complex objects, where several fringe patterns merge, the reconstruction can also be used to determine the source size: the source is smaller than the smallest observable detail. Physically, this form of determination amounts to measuring the smallest visible fringe. Generally, the reconstruction with the best contrast is chosen, the source-to-object distance is determined from this reconstruction, and the source size can be
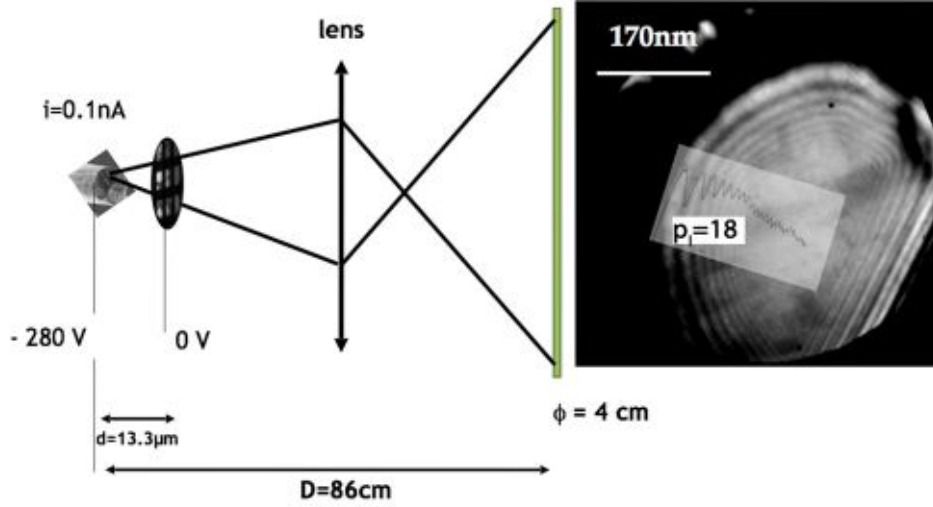
Figure 2: The size of a bulky electron source (so-called celadonite source) is determined by using a lens to enlarge the recording hologram and measuring the smallest detail on the image: the last visible fringe order ($p_l = 18$). Here, the source size is $s < 2.6nm$. Magnification: $G = 235000$, electron source potential $V = -280V$, source-screen distance $D = 86cm$, source-object distance $d = 13.3\mu m$

estimated from the error function applied to the final image. The figure 3 shows this reconstruction, also realized with the celadonite source and giving a source size of below $s < 2nm$.

- Measuring the contrast in an interferometry recording is the most accurate way to deduce the size of the electron source. If a small filament is positively charged, the electron beam appears to come from 2 sources separated by $a$, which depends on the filament charge. Fringes are then regular ($i = \frac{\lambda D}{a}$), with an intensity modulation that results from the sharp cutoff in wave vector direction right after the biprism. The contrast $\Gamma = \frac{I_{Max} - I_{min}}{I_{Max} + I_{min}}$ depends on source size [17]: $\Gamma = sinc\frac{2\pi Ds}{id}$. This method is illustrated in figure 4; to obtain such a contrast ($\Gamma = 0.33 > 0.217$), the size of the source needs to be within the first lobe of the $sinc$ curve. The $sinc$ curve can be turned into a sum, giving: $s = \frac{di\sqrt{1-\Gamma}}{2\pi D}$. Here, the source size is estimated at $s < (1.5 \pm 0.3)nm$.

# 3 An insulating crystal-on-conductor electron source

In early versions of the electron source composed of an insulating crystal (celadonite) deposited on a carbon fiber, crystals were deposited on carbon films. This meant that several crystals would emit but the intensity plotted against the voltage indicated a Fowler-Nordheim regime followed by a saturation regime.
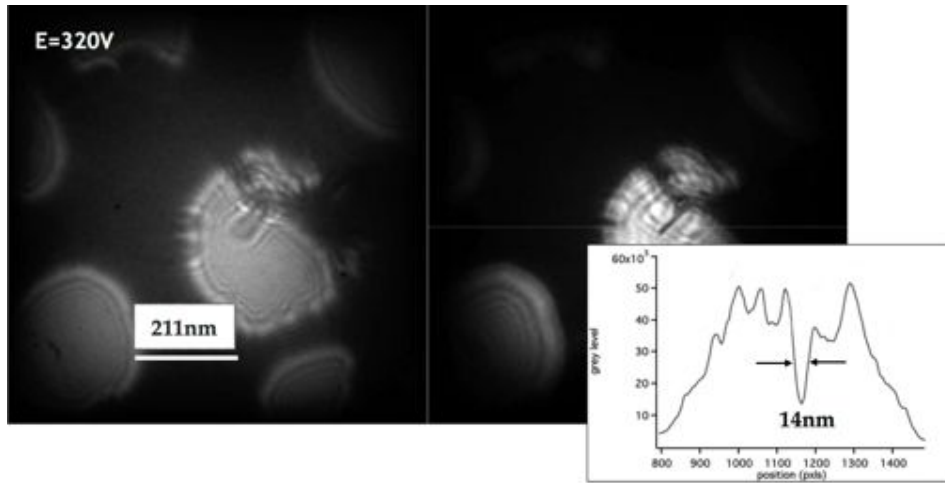
Figure 3: Hologram obtained in a point-projection microscope with a celadonite source and its reconstruction. The inset corresponds to the profile along a horizontal line on the reconstruction. The error function applied to the profile of the "best contrast" reconstructed image gives a source size of $s < 2nm$.
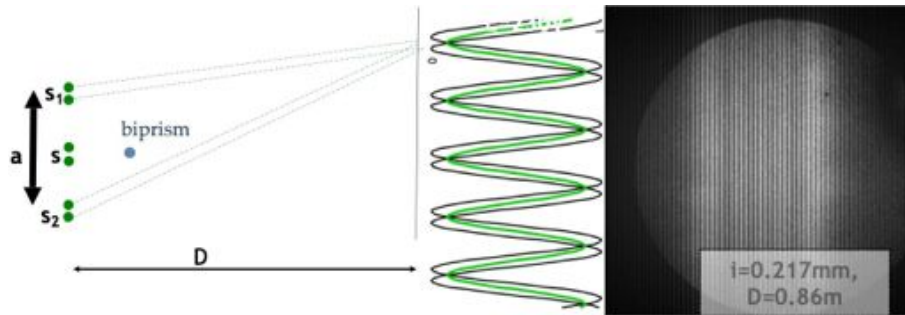


Figure 4: Interferometry experiment carried out with a charged filament using the celadonite source. Electron energy: $E_e = 227eV$, projection distance $D = 86cm$, inter-source distance: $a = 280 \pm 30nm$, source-object distance $d = 15 \pm 3\mu m$, fringe-to-fringe distance $i = 0.24mm$. Contrast $\Gamma$ depends on source size, here estimated at $s < 1.5nm$.

In order to characterize the beam from a single crystal, the intention was to use the point-projection microscope, so the source-object distance had to be small. Thus, insulating crystals are now deposited with a micropipette at the end of a carbon fiber, so that the object is closer to the source. The I(V) curve remains the same, except that the voltage is lower because the shape of the conductive substrate leads to a higher electric field. The macroscopic field responsible for the emission remains the same, in the order of some $V/\mu m$. The crystal is perfectly flat and thin on the rough conductive surface. When the fiber is polarized, the crystal surface charges to a potential different from the fiber,

creating local field enhancement. At nanoscale, the roughness of the conductor enhances the local field. When this local field reaches some $V/nm$, electron emission takes place [6]. However, this source is not an ultra-thin tip; it is situated at the end of a carbon fiber of $\phi = 10\mu m$ diameter, and the approach is therefore limited to some tens of micrometers [9]. For this reason, a new point-projection microscope was realized, comprising a micro-manipulator, a double electrostatic Einzel lens, and a double micro-channel plate detector [10]. These modifications enabled us to achieve a source size of $s = 1.5nm$ according to the interferometric measurement described above. The key was maintaining a minimum source-to-object distance of the order of $d = 12\mu m$, sufficiently comfortable to envisage off-axis holography.

# 4    Conclusion

In summary, the point-projection microscope provides contrast that is directly dependent on the size of the source. This makes it particularly useful for studying sources. It is not always possible to use the simple projection system, but the use of lenses or high-precision detectors has been shown to help increase the resolution. A new electron source composed of an insulating crystal deposited on a conductive fiber has a brightness equivalent to that of conventional field emission sources (ultra-thin metal tip). It is robust, easy to prepare, and has a long lifetime, even at high pressure. To study this source, a special point-projection microscope was developed to meet the challenge of maintaining a minimum source-to-object distance of $d > 12\mu m$. Today, this new type of microscope holds promise for a number of applications, like off-axis holography.

# Acknowledgments

# References

[1] D. Gabor. A new microscopic principle. *Nature*, 161:777, 1948.

[2] R. Morin and H.W. Fink. *App. Phys. Lett.*, 65:2362, 1994.

[3] Nicholas P. Economou, John A. Notte, and William B. Thompson. The history and development of the helium ion microscope. *Scanning*, 34:83–89, 2012.

[4] W. Stocker, H.W. Fink, and R. Morin. Low-energy electron and ion projection microscopy. *Ultramicroscopy*, 31:379, 1989.

[5] Jorge Garcia-Sucerquia, Wenbo Xu, Stephan K. Jericho, Peter Klages, Manfred H. Jericho, and H. Jurgen Kreuzer. Digital in-line holographic microscopy. *APPLIED OPTICS*, 45(5):836–850, 2006.

[6] E. Salançon, R. Daineche, O. Grauby, and R. Morin. *J. Vac. Sci. Technol. B*, 33:030601, 2015.

[7] E. Salançon, Alain Degiovanni, Laurent Lapena, and Roger Morin. From measuring electron charge to exploring particle-wave duality: A new didactic experimental approach. *American Journal of Physics*, 87:194, 2019.

[8] Evelyne Salançon, Alain Degiovanni, Laurent Lapena, and Roger Morin. High spatial resolution detection of low-energy electrons using an event-counting method, application to point projection microscopy. *Review of Scientific Instruments*, 89, 2018.

[9] E. Salançon, Alain Degiovanni, Laurent Lapena, Mehdi Lagaize, and Roger Morin. Preparing a celadonite electron source and estimating its brightness. *Journal of visualized experiments : JoVE*, 153, 2019.

[10] E. Salançon, Alain Degiovanni, Laurent Lapena, Mehdi Lagaize, and Roger Morin. A low-energy electron point-source projection microscope not using a sharp metal tip performs well in long-range imaging. *Ultramicroscopy*, 200:125–131, 2019.

[11] R. Morin and A. Gargani. *Phys. Rev. B*, 48(9):6643–6645, 1993.

[12] E. Salancon, Z. Hammadi, and R. Morin. A new approach to gas field ion sources. *Ultramicroscopy*, 95:183188, 2003.

[13] Z. Hammadi, M. Descoins, E. Salancon, and R. Morin. Proton and light ions nanobeams from field ionization of water. *Applied Physics Letters*, 101:243110, 2012.

[14] A. Degiovanni and R. Morin. Interferometry with low energy electrons. *J. Vac. Sci. Technol. B*, 13(2):407–409, 1995.

[15] J. Bardon, V. Georges, A. Degiovanni, and R. Morin. Improved low energy electron projection in-line holograms reconstruction: application to the holograms of a tungsten tip. *Micron*, 33:493–497, 2002.

[16] Tatiana Latychevskaia. Holography and coherent diffraction imaging with low-(30250 ev) and high-(80300 kev) energy electrons: History, principles, and recent trends. *Materials*, 13:3089, 2020.

[17] Max Born and Emil Wolf. Principles of optics: Electromagnetic theory of propagation, interference and diffraction of light. *Cambridge University Press*, 1999.